Electrical Power and Energy Systems 105 (2019) 1–16

Contents lists available at ScienceDirect

Electrical Power and Energy Systems

journal homepage: www.elsevier.com/locate/ijepes

Dynamic simulation of induced voltages in high voltage cable sheaths: Steady state approach

Matilde Santos[a,*], Miguel Angel Calafat[b]

[a] Computer Science Faculty, Universidad Complutense de Madrid, Spain
[b] Red Eléctrica de España, Spain

ARTICLE INFO

Keywords:
Modeling
Simulation
Underground cables
Cable sheath
High voltage
Induced voltages
Steady state

ABSTRACT

This paper presents a novel approach to the modeling of high voltage underground cables. Its main contribution is that it considers induced effects. Indeed, it incorporates the estimate of induced voltages and currents in cable sheaths in steady state due to the nearby cables and sheaths, for different types of sheaths connections and for various single-phase short-circuit configurations and three-phase short-circuits. Furthermore, it allows multiple circuits to be coupled automatically in a simple way. An intuitive and friendly simulation tool has been implemented that allows the automatic generation of multiple coupling circuits and to calculate all these induced effects caused by the connection of the sheaths and the distance between cables. It has been validated by comparing it with the expected theoretical data and to other simulators with satisfactory results.

1. Introduction

Objections to the construction of overhead power lines (OHL) are becoming increasingly common. This is influenced by several factors, such as their visual impact, strong social opposition, the difficulty of carrying out the relevant expropriation of land within the time and cost constraints imposed by the project, etc. This is happening not only in urban environments where space restrictions make clear that overhead technology is impossible, but also occurs increasingly in rural areas. Besides, high voltage cables have an insulation layer, so electroshock and short circuit risks of high voltage underground cable lines are lower than overhead lines. For all these reasons, in recent years we have seen an improvement in the technology of the manufacture and installation of underground insulated high voltage cables [1].

However, this solution has also drawbacks; the cost of an underground cable of the same length and power transmission capacity than an overhead one can be up to 5.6 times higher for the level of 400 kV, although for 150 kV is comparable in price. In addition, underground cables can cause environmental problems by obstructing runoff and the effect on the underground animal habitats.

Moreover, from a technical point of view, electrical calculations for high-voltage (HV) underground cables are very complex and have a number of electrical characteristics that make them very different from those for overhead transmission lines [2–4]. Although a great deal of research work on PD based cable insulation monitoring, diagnostics and localization has been published in recent years on medium voltage (MV) cables, few of them are found on cross-bonded HV cable systems [5,6].

Besides, the sheaths of these insulated cables are bad conductors and generate magnetic fields that originate induced voltages. Then, depending on the type of connection to ground of the sheaths, currents are generated which in turn also induce voltages in nearby sheaths. Indeed, the sheath current generated on metallic sheath can cause electroshock for human, cable fault and reducing of cable performance. These effects must be considered as they influence both line transport capacity and the design of the protections.

Therefore, if the sheath current of high voltage underground cable line is determined before this underground cable is installed in the project phase, the required precautions can be determined according to this estimated value. That is why modeling and simulation are so useful tools. But the modeling of these circuits is not easy, indeed many factors influence the voltages and currents and thus, formulation of the sheath current is difficult and complex [7].

The first objective of this work is to mathematically model and then simulate the voltages induced in insulated cable sheaths of every kind and configuration, in order to visualize their magnitudes and phase angles. It is worthy to remark that the dynamic simulation must have into account how each element influences the other. That is, it is not just to replicate different circuits, but to estimate how the electrical magnitudes of the entire system are affected since a power line behaves

* Corresponding author at: Computer Science Faculty, University Complutense of Madrid, C/ Profesor García Santesmases 9, 28040 Madrid, Spain.
E-mail addresses: msantos@ucm.es (M. Santos), mcalafat@ree.es (M.A. Calafat).

https://doi.org/10.1016/j.ijepes.2018.08.003
Received 19 January 2018; Received in revised form 24 July 2018; Accepted 9 August 2018

differently if another cable or even two or more cables are near enough.

This dynamic modeling is required as the coupling effects influence energy transportation and the design of the electrical facilities. Even more, the induced voltages and currents have an influence on sheath circulating loss, which increases the thermal resistance of cable and then reduces the permissible current. These effects may also cause damage to the cable and to the maintenance personnel [8].

To achieve this goal a simulation tool has been developed. It breaks down the various components of these voltages and enables, in design time, the visualization of different parameters (section cables, grounding resistors, connection settings, line lengths, etc.) that affect the voltages. These effects depend on the connection of the sheaths and the distance between wires. This is important because many of the papers that discuss cable modeling for long high-voltage ac underground cables do not focus on these induced effects. In addition, we are interested in developing an easy and friendly simulator which allows to obtain results in a quick way, in order to roughly check if the measures are right and to properly plan a project with further details.

Many papers are focused on some spurious effects at high frequencies, specifically, skin and proximity effects. They mainly affect the transport capacity of the cables. Although they may not play a major role for lower frequencies (below around 10 kHz), there are significant deviations between the simulation and the measured results at high frequencies. Some works use EMTP (ElectroMagnetic Transients Program), such as in [9,10], to calculate them. In [11] authors also use EMTP to investigate some basic and qualitative characteristics of the proximity effect depending on the current directions on the conductors. In [7], authors try to forecast the sheath current using statistical methods and simulate high voltage underground cable lines. In a recent paper by Brito et al. [12], the influence on the resistance and inductance per unit length matrix elements of the proximity and skin effects are considered. An analytical methodology based on the magnetic vector potential formulation where appropriate boundary conditions allow the magnetic field solution to be obtained is applied to three-phase underground cable with conductive sheaths. From the point of view of distribution networks reliability, the work reported in [13] characterizes the fault process in underground cables using a time-domain system model and a statistical parameter estimation strategy.

Other papers that also include the proximity effect in the cable models are, for instance [14], where a systematic approach for calculating electrical per-unit-length parameters of signal cables by the finite-element method is presented. Techniques based on FEM are used. Paper [15] takes into account the proximity effect arising from currents mutually induced by nearby conductors which, in turn, modify their internal current density distribution and, hence, their impedance. They apply a semi-analytical method base on conductor partitioning. MoM-SO (Method of Moments-Surface Operator) can also capture accurately the skin and proximity effects by solving Maxwell's equation in 2D [16,17]. They propose a surface current approach for systems of round solid and tubular conductors, allowing to model realistic cables with tubular sheaths, armors, and pipes. These techniques compute proximity-aware impedance parameters which can be used to compute voltages/currents. In [18], after numerical simulations, authors conclude that proximity effect will lead to uneven current distribution in cables.

Our work is not focused on the proximity effects, so important for line transport capacity, but on the induced currents and voltages caused by the fact that cables and sheaths are nearby. Besides, we work on the steady state, where the proximity effects are not relevant. Indeed, we have calculated the proximity effects to see how they affect the induced voltages on screens. This has been useful to verify that these effects on a hollow conductor such a sheath are negligible. For a 220 kV trench with standard conductors, the skin effect would cause an increase around 0.0006% and the proximity effect an increase of approximately 0.8% in the sheath ohmic resistance. In a more restrictive case (for example, if the three cables are closed together), the proximity effect would increase the resistance of the sheath by 6% (modeling it as an impedance, just to estimate it). Thus, in the most unfavorable case (cables attached), the variation on the effective output voltage of the sheaths is about tenths of a volt. Therefore, the important part of the sheath voltage is induced and it is not caused by the current flow.

The paper [19] presents a review on analytical techniques used to calculate induced sheath voltage in metallic sheaths of underground cables and overhead lines. The findings indicate that when two parallel cables are fairly close together then the electromagnetic coupling effect between the adjacent cables is difficult to calculate.

Another contribution of our work is that it allows multiple circuits to be coupled automatically, without the need to manually define each individual coupling. Other papers found in the literature do not allow this dynamic modeling or are focused on other aspects, such as the transient characteristics of grounding systems used in under-ground distribution power cables [20,21]. In [20,22] a simulation tool developed with Matlab/Simulink is proposed to prelocate insulation faults affecting electrical single-phase cables by using measurements of voltage and current. In fact, simulation has been typically used for fault location on cross-bonded cable systems, using sheath currents [23]. In [24] authors only deal with single-core cable line and an additional conductor that are reduced to a simple equivalent π-circuit and modeled by an analytical approach. The same configuration is presented in [25], where the effect of configuration of high voltage power cables on induced voltages in their metallic sheaths is computed. In other papers, such as in [26], or in [27], several cables are generated, including mutual coupling between them. In the first case, this is based on a general formulation of impedances and admittances of single-core coaxial and pipe-type cables, allowing to handle a coaxial cable consisting of a core, sheath and armor, a pipe-type cable of which the pipe thickness is finite and an overhead cable. In the paper by Patel and Triverio [27], MoM-SO technique automatically include mutual coupling via ground return impedance between cables.

Back to our proposal, the developed model emulates the performance of the different configurations on the basis of the power line data introduced by the user. The simulation tool is designed and implemented with SPICE [28]. Unlike other approaches, this way of modeling allows greater speed of development because it is dynamic and the model itself does not appear in SPICE language until the end. If an element by element modeling is performed using a graphical environment (like Simulink or graphics-based environments such as Schematics SPICE), it is not possible to connect a line with another efficiently if you do not have a module for a dual circuit. Obviously, this applies to a triple circuit, quad circuit, etc. Although some newer versions of certain simulators allow the ability to couple multiple circuits, it is at the expense of laboriously defining each connection manually, a task performed automatically by our software. For this reason, it is common in professional environments to see a single circuit line being modeled instead of two lines (when applicable), with the assumption that having a double circuit will not change the induced voltages in the first circuit in the event of a short circuit [29].

The modeling carried out in this work is quite consistent with reality in terms of modeling the underground line with all the parameters that play an important role in calculating the induced voltages. It has been validated by comparing it with the expected theoretical data and to other well-known simulators with satisfactory results. The program works well and it is simpler and more intuitive than other commercial ones. Even for steady state, it improves the usability of other general simulators, as far as we know, taking into account aspects not included by other programs, such as the simulation of induced currents and voltages.

The structure of the paper is as follows. Section 2 briefly describes the components of an insulated high voltage power cable and the possible connections between sheaths. Section 3 presents the calculation and modeling of the induced voltages. Section 4 shows the software tool developed and simulation results are then discussed to test and validate the proposal. Conclusions end the paper.

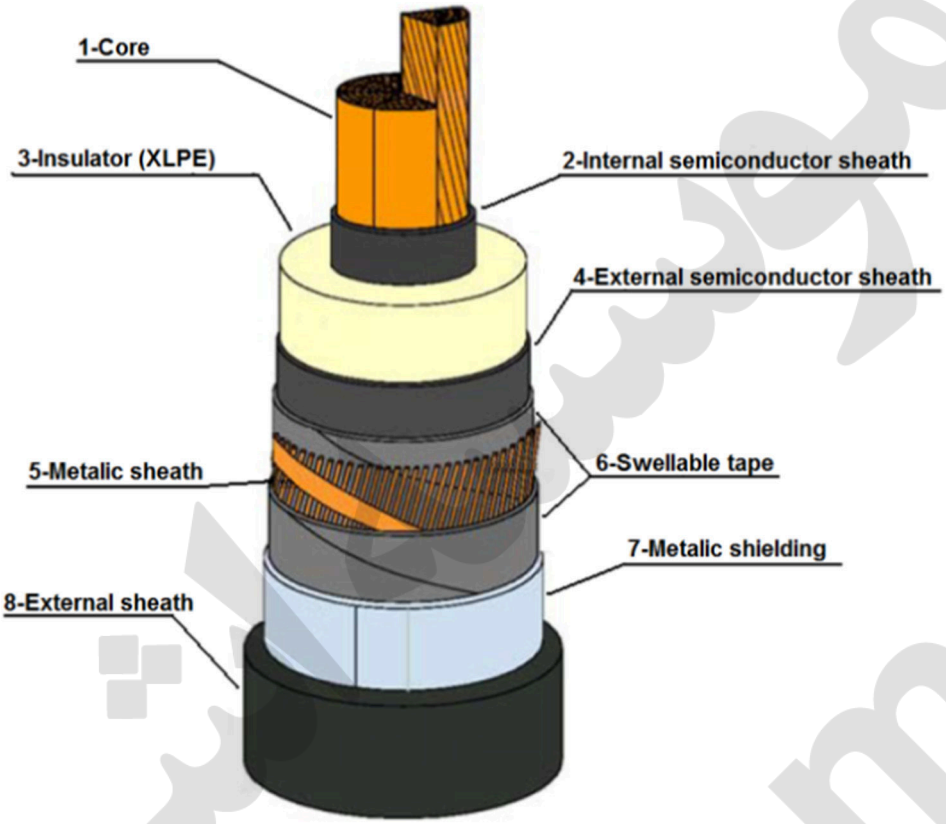

Fig. 1. Components of an insulated high-voltage cable.

2. Brief description of insulated cables and bonding methods

Nowadays there are different technical solutions which allow very high current ratings in undergrounded insulated cables [30]. Electrical cables can be classified according to various criteria such as voltage, use, number of phases and the type of insulation. Insulated cables have a sheath made of conductive material which completely insulates the electric field; but when this material is crossed by the magnetic field generated by AC current, voltages and/or currents are induced in those same sheaths. These voltages and currents must be carefully calculated because they affect both the power handling capacity of the transmission line and the design of the protections to be installed. In addition, depending on the type of sheath and grounding connections, currents will be produced which, in turn, will also induce voltages in nearby sheaths [31].

This paper will refer in particular to single core cables with XLPE insulation for voltages greater than or equivalent to 66 kV and for underground (as opposed to underwater) use. The general composition of these cables is shown in Fig. 1.

Three electrical phenomena are especially notable in the conductor behavior: the ohmic loss, skin effect and the proximity effect loss. But they are not in the scope of this work.

Regarding the sheath, it is also an active conductor for the capacitive currents in the insulation, currents induced by the magnetic fields of nearby cables (depending on sheath's connection), and zero sequence current, draining them all to ground. In practice this feature enables dimensioning of the metallic sheath. Furthermore, this implies the need to ground it, and carefully study the design of this connection. That is why it is important to estimate these induced effects in order to the choose the correct cable section that can handle the required transport capacity and make some other considerations about the protection of the electrical installations.

2.1. Bonding methods

If voltage is induced in a conductor that forms part of a closed circuit, then current will flow, hence the type of cable shield connection plays a decisive role in the voltages and currents that may be present. Sheaths of conductive material crossed by magnetic alternating fields produce induced voltages and/or currents too. These voltages are also determined by the type of sheath connection and the proximity between the lines [32]. Different and complex combinations can be formed using the three basic types of connections that have been implemented in our model. These are:

Solid Bonding (SB) or Both Ends: as its name implies, the sheaths are earthed at both ends of the line or the section in question. This method of grounding sheaths is rarely used in high voltage lines.

Single Point (SP): in this type of sheath connection one end is earthed and the other is not. In fact, this latter end is earthed through sheath voltage limiters (SVL). It is important to have a parallel ground continuity conductor (ecc) grounded at the ends, in order to minimize circulating steady state currents and, therefore, losses. Its main disadvantage is that a voltage is induced in the side of the surge arrester. This voltage is proportional to the length of the line and, in a steady state, its strength could be dangerous to people.

If a short-circuit occurs, the induced voltages may prove hazardous even for the cable cover (jacket) which is usually designed to withstand 10 kV in power transmission cables of 66, 132 and 220 kV. This is the reason why the line is protected with surge arresters [33].

Cross Bonding (CB): A CB section is grounded at both ends. Each CB section is formed by three elementary segments of equal length (insofar as possible). Sheaths are transposed at every joint bay so that the sheath that was associated with phase 1 in the first segment, goes to phase 2; the sheath associated with phase 2 goes to phase 3, and the sheath associated with phase 3 goes to phase 1 (Fig. 2). It is customary to refer to phases as R, S and T, or 0, 4 and 8, as an indication of the phase

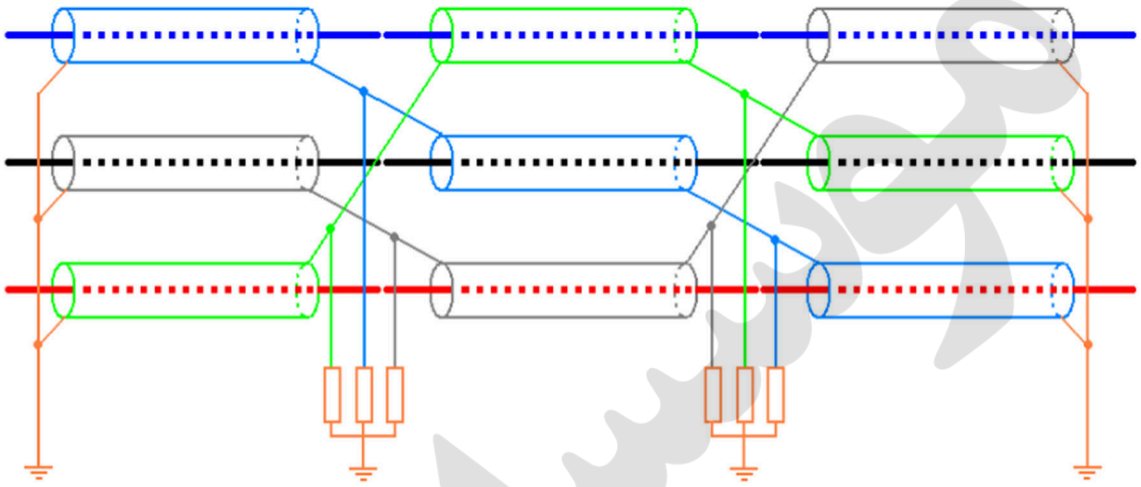

Fig. 2. Cross bonding grounding system.

displacement angle in time units, although this depends on each company. This paper will use 1, 2 and 3 for simplicity.

Sheaths will be transposed at the two joint bays in the CB section. If the lengths are equal (and the currents are also equal), then the induced current in sheath 1 of section 1 will be partially compensated by the induced current in the same sheath (remember that it is transposed) in section 2, and will be finally canceled by the voltage induced in section 3, in the case of a trefoil formation.

3. Estimate and model of insulated cables circuits

The final goal of this work is to estimate and shown induced voltages in underground power lines. The following models have been developed to obtain and simulate these voltages and currents in insulated cables.

3.1. Induced voltages estimate in insulated cables

Carson's empirical equations [32,33] are used in this work to estimate the induced voltages (instead of the more complex and accurate Pollaczek impedance formulas). Our goal is to obtain a first estimation of some effects on the underground cables, mainly the voltages and currents in the sheaths. According to the order of magnitude of these effects, it could be convenience to carry out a more accurate and exhaustive analysis but it may not be necessary in some real installations. That is why we have used approximate formulas for ground impedance [34]. Although more accurate formulas could have been applied, we considered that the approximation is good enough for our purpose. Carson's equations allow us to calculate the mutual impedances between the phase conductors and sheaths, between the sheaths, and the self-inductance in the individual sheath as follows:

$$Z_{c,p} = \frac{\omega \cdot \mu_0}{2}\left(\frac{1}{4} + j \cdot \frac{1}{\pi} \cdot \ln\left(\frac{D_e}{r_{c,p}}\right)\right) \quad (1)$$

where

$Z_{c,p}$: is the induced impedance between conductor and sheath (Ω/m)
ω: is the angular frequency (rad/s)
μ_0: is the vacuum permeability ($4\pi 10^{-7}$ H/m)
$r_{c,p}$: is the distance between conductor and sheath (m)
D_e: is the distance to the equivalent ground conductor (m)

Certain considerations are necessary for these calculations. First, the ground return equivalent, D_e, is calculated by the following equation,

$$D_e = \frac{1.85}{\sqrt{\frac{\omega \cdot \mu_0}{\rho}}} \quad (2)$$

where ρ is the ground resistivity (Ω m).

As said, $r_{c,p}$ is the distance between the center of the conductor and the center of the sheath whose mutual impedance must be calculated. If the coupling between two sheaths is to be obtained, the formula is the same because the distance between their centers is equal to that between the center of the conductor and the center of the sheath.

If what is going to be calculated is the mutual impedance between a conductor and its own sheath, as the distance between their centers is zero, $r_{c,p}$ is equal to the length weighted geometric mean radius (GMR) of the sheath. This geometric mean radius of a sheath (a hollow conductor) is approximately equal to the outer radius of the sheath and, therefore, it can be used with a small error.

When calculating the characteristic impedance of a solid conductor (for example, the parallel ground continuity conductor), then $r_{c,p}$ is equal to the length weighted geometric mean radius of the conductor. This value can be calculated by multiplying the outer radius of the conductor, r_{ext} (m), by the factor $e^{-1/4}$.

In short, the formula used in this study to calculate induced impedances is always the same, and it uses the distance between the centers of the two elements under consideration. The conductor-sheath distance is exactly equal to the sheath-sheath distance. When calculating the sheath-sheath impedance of the same element (sheath1-sheath1, sheath2-sheath2, etc.), then the distance to consider, instead of being zero, is the radius of the sheath (the same applies in the case of the conductor and its own sheath). As for the parallel ground continuity conductor, as a solid conductor, the distance to be considered is the geometric mean radius.

When modeling, particular care must be taken for a given element (sheath or parallel ground continuity conductor) because the estimate of the induced impedance will have to be added to the natural impedance of the element itself, which is indicated in the technical data sheet. Then the induced voltages will be obtained depending on the specific sheath connection.

Indeed, all elements where current is flowing will induce voltages in all the close elements. In a three-phase circuit, conductor 1, 2 and 3 will induce voltages on sheaths 1, 2 and 3. Also, if the connection type is such that it allows current flow, then the currents in sheaths 1, 2 and 3 will generate induced voltages on the others sheaths and on themselves. The same will happen to any wire close to these elements. Therefore, these calculations generate a system of equations that grows quickly.

Due to lack of space, this paper formulates neither that calculation nor the single phase short-circuits analysis but all of them have been implemented in the model.

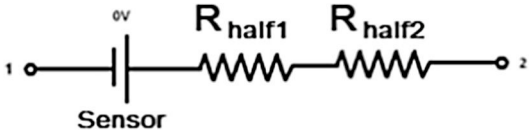

Fig. 3. Conductor model.

3.2. Components model

The main elements of the model and how the induced voltages are obtained by our simulation tool are described in this section.

There are some well-known conductor models, as the one proposed by John J. Grainger and William D. Stevenson based on its internal inductance [34]. However, we use another approach since our goal is to calculate the induced voltages in the cables sheaths and the relationship (phase displacement angle) between the currents/voltages of one another. Indeed, the inductances are not included in our model because the basis is the conductor current. This is the starting point for all the calculations. If there were certain lag between voltage and current on the conductor, it can be neglected in the calculation of the induced currents and voltages.

Thus, the starting point is the current flowing through the conductor and not the supply voltage. Put in another way, the currents do induce voltage in sheaths; so, for a given current, the induced voltages will be virtually identical, irrespective of the line voltage.

In short, *conductors* will be modeled only by their ohmic resistance. Therefore, the selected conductor model comprises two resistors in series (Fig. 3), instead of one in order to be able to access any point of the conductor. This point is used for modeling the capacitor that represents the stray cable capacitance. The voltage source, at the left side of the conductor model (Fig. 3), is necessary because in Spice voltage sources can be used as sensors and they measure the current that passes through them.

The value of each of the resistances will be equal to half the value of the resistance of the conductor all along its length.

At this point, the program will have the value of the current flowing through the conductors, which will be the starting data.

To induce voltage in a given conductor, whether a sheath or an earth continuity conductor (ecc), the mutual impedance between the inductor element (*killer*) and the element receiving the induction (*victim*) must have been previously calculated. This calculation has been described in Section 3.1. Once the mutual impedance and the current flowing through the conductor are known, the induced voltage is calculated by simply multiplying one by another.

In the simulation scheme, this is done by designing an "isolated" electrical circuit with two components: the calculated mutual impedance and a current dependent current source (CDCS), with the value of the current measured in the conductor. This isolated circuit is shown in Fig. 4 (central part). The term "isolated" means it does not have any physical connection to other parts of the model. That is, it is not part of the electrical model of the conductor, neither of the electrical model of the sheath, but it is the model that calculates the induced voltage from one to the other.

The voltage in that current source will be the induced voltage per unit length on the sheath. It is related to the conductor model and to the sheath model through voltage dependent sources, that depends on other magnitudes of those models.

At this point the next step is to apply the induced voltage on the sheath. This is done by inserting a voltage dependent voltage source (VDVS) in the electrical model of the sheath. The value of this source will be the value of the CDCS cited before, multiplied by the length of the considered circuit.

In summary, as it is shown in Fig. 4, the sensor of the conductor between nodes 1 and 2 is represented at the top of the figure, as part of the electrical model of the conductor. At the central part of the figure it

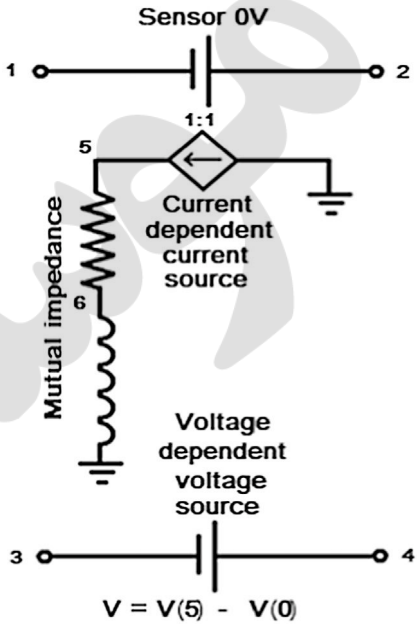

Fig. 4. Electrical model of the voltage induced in any element affected by mutual impedance.

is possible to see the "isolated" circuit where voltage per unit length is calculated between nodes 5 and earth. Finally, at the bottom, the voltage dependent voltage source that will be inserted in the sheaths model is drawn.

The *sheath model* is a combination of the above elements. Besides, two resistors are used to model the sheath resistive effect and two inductors represents its self-inductance. The value of the resistors is the resistance of the sheath at 50 Hz at service temperature, taking into account the appropriate correction factors. Again, a sensor is located at the input of the sheath in order to measure the current flowing through it.

Obviously, what has been shown for a conductor and a sheath has to be extrapolated due to the fact that the currents through all the conductors and sheaths induce voltage in all the sheaths; that is, the sheaths (and ecc) will have in their model as many voltage sources as inductor elements there are.

Fig. 5 shows an example of the model of a single circuit sheath without parallel ground continuity conductor (ecc). The voltage sources represent the voltages induced by the currents through the three phases (cond1, cond2 and cond3) and by the currents through the other two sheaths (sheath2 and sheath3). The self-inductance is already modeled in the coils.

Although the *cable capacity* is not very relevant when calculating the induced voltages, it is also true that there will be such capacity current between the conductor and the sheaths. Some approaches ignore this effect [33], but it may be important in same cases. Therefore, we have modeled what it is called an advanced condenser that will help to estimate, if necessary, power losses. It includes, besides its self-capacity, other capacities, inductances and resistances to simulate its real behavior (Fig. 6). The values of these other components are carefully selected so that the module of the capacity is about 95% of an only condenser, and the angle generates a phase shift of 78° instead of the 90° of an ideal one.

The values are calculated as follows.

$$L_{ser} = \frac{1}{1.5 \times 10^5 \cdot \pi^2 \cdot C} \quad R_{ser} = \frac{1}{500 \cdot \pi \cdot C} \quad C_{par} = \frac{C}{2 \times 10^{22}} \quad R_{par} = \frac{3 \times 10^6}{\pi \cdot C} \tag{4}$$

where L_{ser} is the serial inductance (H), R_{ser} is the serial resistance (Ω), C_{par} is the parallel capacity (F), R_{par} the parallel resistance (Ω) and C the

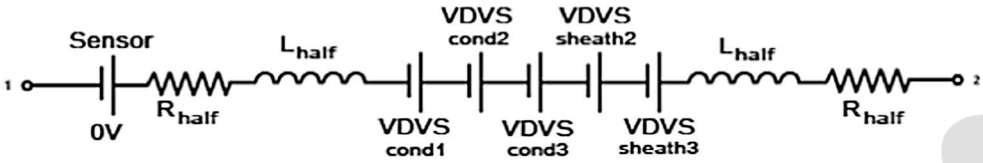

Fig. 5. Model of a single circuit sheath without parallel ground continuity conductor.

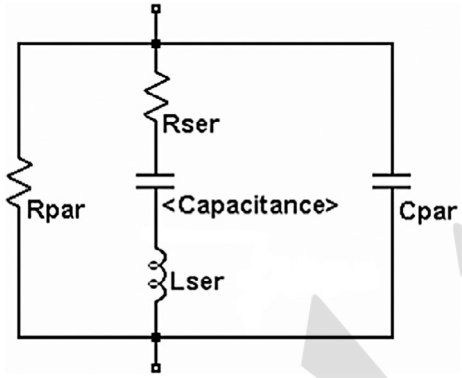

Fig. 6. Advanced capacitor model.

capacity of the original capacitor (F).

For simplicity, the stray capacitance is represented as a capacitor in the following figures, although it is a bit more complex than that, as it has been shown.

In Fig. 5 we still have to determine the value of the voltage sources. This is part of the modeling itself and it is not a parameter that is set before running the simulation. Thus, in a rigorous way, it cannot be said that what it is so far presented is really a cable model, since it is necessarily associated to the mutual coupling impedances with all the elements that induce voltage. This is due to the fact that the cable induced voltages will depend on the other cables close to it. That is what is shown in Fig. 7. In the model, FiPi represent the phase Fi and Pi sheath mutual impedance.

Even more, the induced voltage circuits involve certain current-dependent current sources; so, the model of a cable also depends on the other cables that are close to it. Therefore, the model of a single-circuit three-phase line without ecc (the simplest possible model) would be as shown in Fig. 8.

All the induced voltages in each small circuit are different from each other. Each of them corresponds to an element of the mutual impedance matrix. In fact, the distribution of Fig. 8 roughly indicates the element to which the reference is made. Thus, by rows from top to bottom, references are made to sheath 1, 2 and 3, respectively; while columns refer to phase 1, phase 2, phase 3 and then to the two sheaths left, which will be sheath 2 and sheath 3 when sheath 1 is considered, or sheath 1 and sheath 3 when sheath 2 is taken into account, etc.

If the circuit has a parallel ground continuity conductor (ecc), the model -as in Fig. 5- will have, in addition to a pair of resistances and a pair of own inductances, an induced voltage source (sensor) for each phase and sheath and, therefore, six voltage sources.

Besides, all sheaths should add one more voltage source, which models the induced voltage in the sheath resulting from the current through the ecc. Clearly, each voltage source must be associated with a small loop formed by the mutual impedance between the ecc and the specific sheath, and the current source determined by the current through the ecc.

Therefore, for a single circuit with an ecc, six voltage sources must be used in each branch to model a sheath. If there is a double circuit, all the second circuit phases, sheaths and ecc will induce voltage in all the first circuit elements (sheaths and ecc) and vice versa. Hence, for two circuits with parallel ground continuity conductors (ecc), there must be thirteen voltage sources for each sheath (the three phases of the two circuits, the other two sheaths of the circuit itself, the three sheaths of the other circuit and, finally, the two ground continuity conductors). That is, the model of a double circuit is not obtained by directly replicating a simple circuit model twice, but it changes and expands rapidly.

As an extreme case, if nine circuits are placed in parallel with double ecc each (this is the maximum that our developed program supports) there would be 71 voltage sources in each sheath. But as the distance between circuits increases, the magnetic coupling decreases to such an extent that it can be neglected. So, it is up to the user to decide

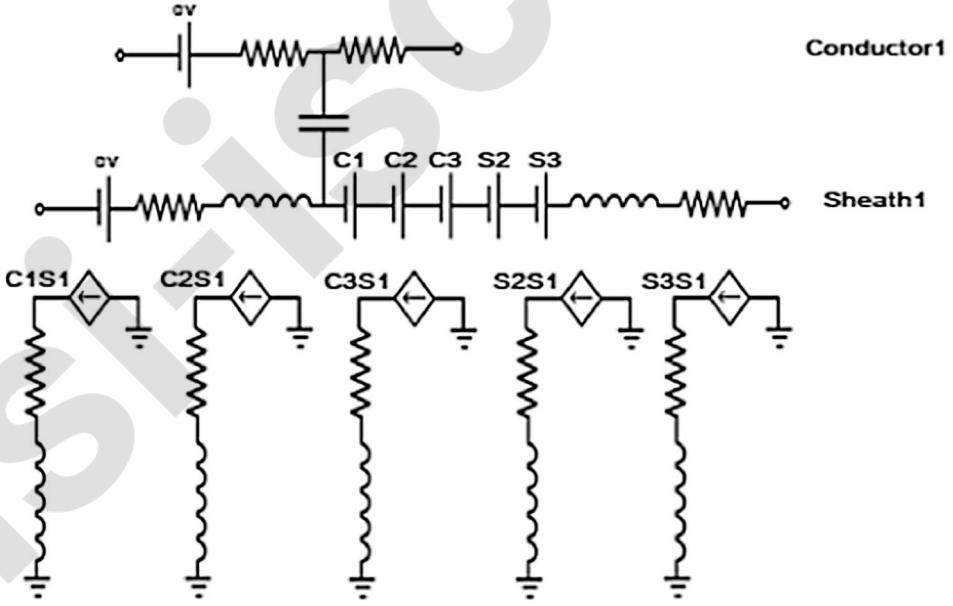

Fig. 7. Model of power cables in a single circuit without parallel ground continuity conductor.

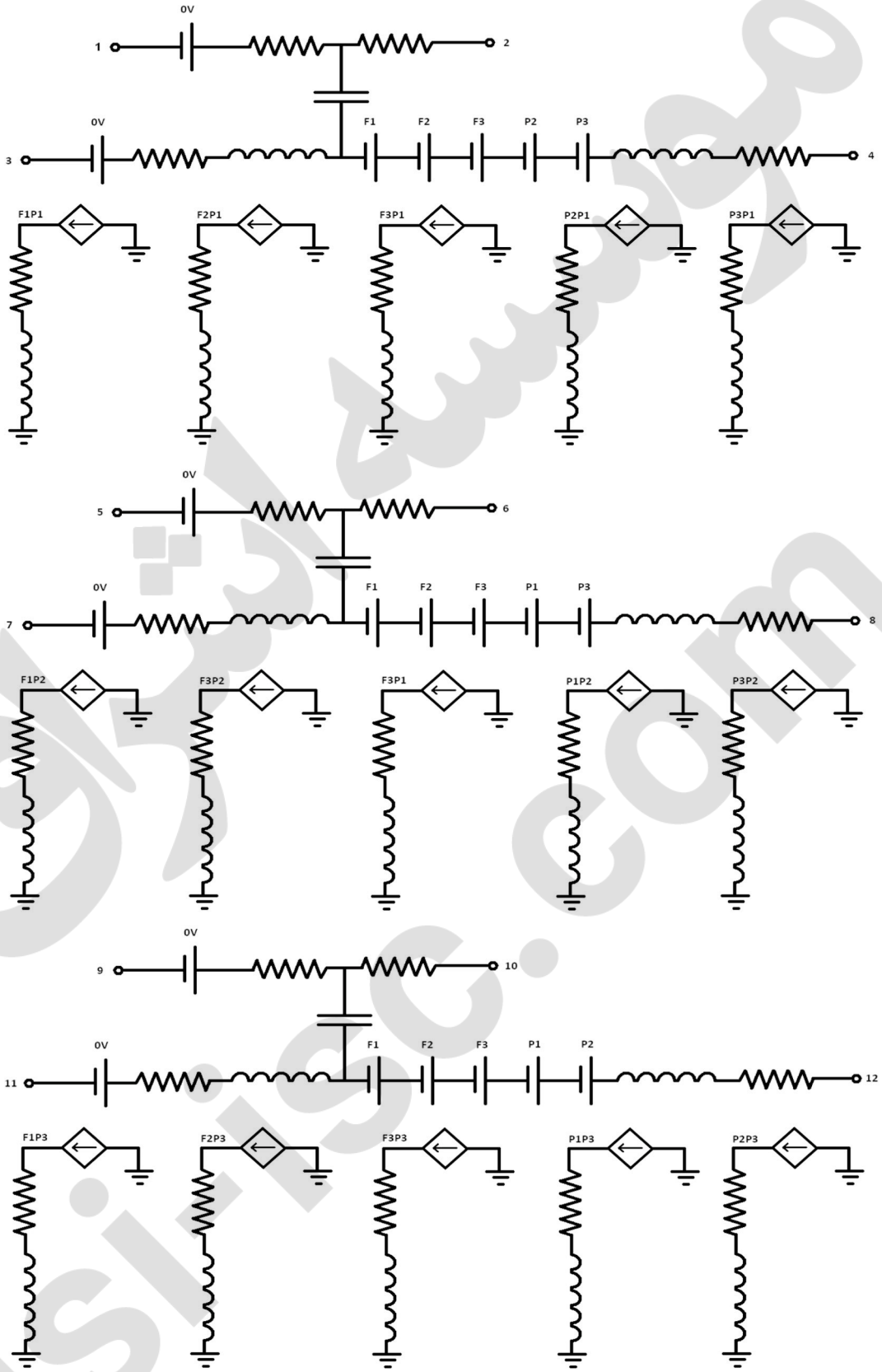

Fig. 8. Model of power cables in a single circuit without parallel ground continuity conductor, including all the killers and victims, and all the isolated circuits that calculate induced voltages.

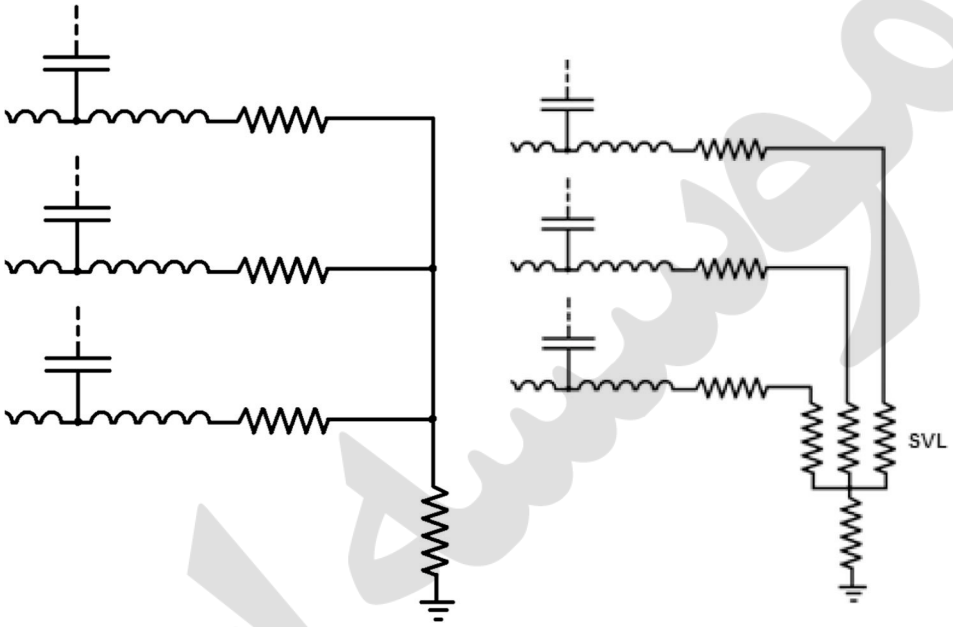

Fig. 9. Solid bonding (left) and single point connections (right).

whether to make use of this calculation as it may not add any significant information beyond the consideration of three circuits.

Finally, it must be said that once you have the electrical model, you will have to connect the sheaths to ground through the corresponding earthing resistors, taking into account the type of connection of the line (cross bonding, solid bonding, single point). In this way the circuit is completed and the voltages and currents in the sheaths can be computed correctly.

In the developed program this process goes on in the background, thus the user is unaware and does not have to make further consideration, but it is taken into account.

3.3. Modeling the grounding sheaths connections

The three types of sheath to ground connections (Section 2.1) have been implemented. In the first one, solid bonding (SB), the sheaths are directly connected to earth. It is modeled by a resistance (Fig. 9, left).

In the Single Point connection (SP), one end is earthed and the other is earthed through sheath voltage limiters (SVL). These can be modeled as very big resistances. Indeed, it is ideally equivalent to an open circuit. In this work, in order to avoid certain problems in the simulation, we have connected the sheaths to a very high value resistor (1 MW) (Fig. 9, right).

Moreover, another connection has been implemented. It consists of grounding a segment of the sheath directly to the next segment. Although it is like if there were not any connection point, it makes easier the modeling of two parallel circuits if one of them changes its configuration. The sheaths connections are kept the same in this case.

3.4. Modeling the load, power and short-circuits

The output variable in these models is the current, both for steady state and for shorts circuits. The power source has been modeled as three-phase star electric current sources 120° shifted (Fig. 10, left). The neutral of the star configuration is connected to the local ground of the sheaths; i.e., it is considered that ground of sheaths and sources is the same.

Regarding the loads, they are modeled so that the terminal voltage is the nominal. Although the voltage does not play an important role in these types of problems, a resistance can model it and the representation is more accurate. Again, the neutral of the three-phase load is connected to the same ground of the sheaths (Fig. 10, right).

Different short-circuits have been also implemented. They are briefly described.

(a) Three-phase fault is modeled by setting the required amplitude to the AC voltage sources so that the RMS short-circuit current flows. As already mentioned, the load values are reduced the same proportion the current increases in order to keep the voltages to their nominal values.
(b) Close phase fault in semi-siphon: it consists of increasing the amplitude of the current source and reducing the phase load in the same proportion. This is possible because of the loads and sources are connected to the same ground.
(c) Distant phase fault in semi-siphon: in the worst case, the total current is injected directly into the ground. But the user may have an interest in modeling not only the worst (always recommended) case but other cases less restrictive. For instance, it may be known that the fault cannot be considered so distant. Therefore, a reduction factor between 0 and 1 has been implemented in our model to simulate any possible case (Fig. 11, left).

A zero voltage source is inserted into the neutral point of the load as a sensor. A current source dependent on the current of the sensor, with a gain between 0 and 1, is also inserted between the sensor and the ground. If this gain is 1, all the current flowing through the neutral is shunted to ground, thus conforming distant failure modeling. If the value of the gain is 0, all the current in the neutral is injected into the local ground of the underground section through a coupling resistance of negligible value, then modeling a near fault. The intermediate values are degrees of freedom that the user can use to configure the different cases.

(d) Close phase fault in siphon: the siphon effect is similar to the far end, but from the opposite point of view. Indeed, in this type of fault all the current of the short circuit that returns to the source does it directly from ground (or from the local substation ground) and not from the local ground of the underground section. Thus, the model of this fault is similar to c) (Fig. 11, right). Again, as in the previous case, the program gives the possibility of reducing the siphoning by a factor between 0 and 1. This value is given by the gain of the source. All the current that is not injected from this

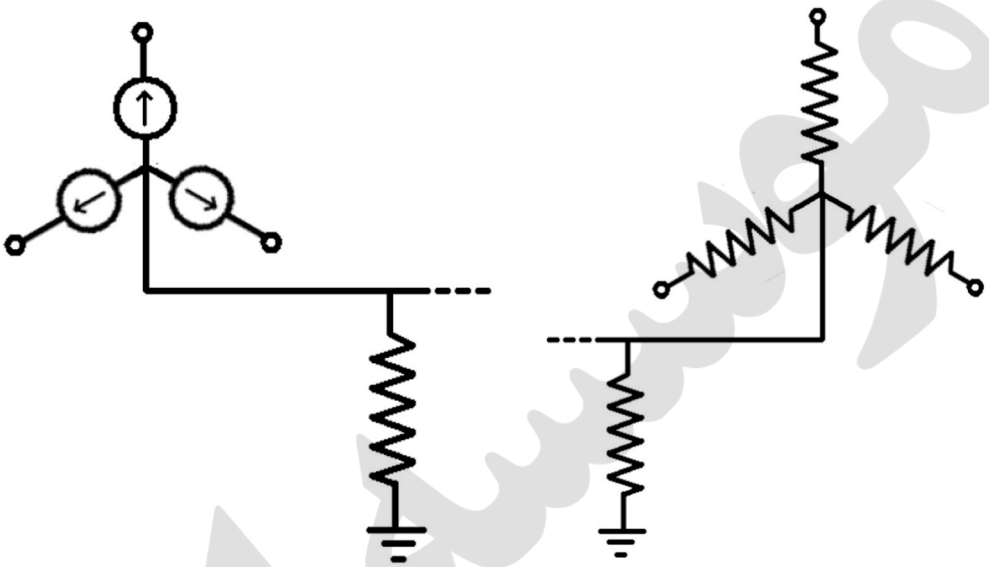

Fig. 10. Three-phase power source (left) and load (right).

source will have to return through the sheaths or through grounding. If the gain is 1, then there is a fault in the siphon; if it is 0, then the fault is in semi-siphon.

(e) Distant siphon fault: the model of this type of failure is a combination of the two previous ones. A reduction factor can be inserted to take into account the different effects.

4. Simulation tool and model validation

The simulation tool here developed was implemented using Excel VBA and LT Spice IV [28]. It is very intuitive and user-friendly. The main screen is shown in Fig. 12. All the parameters can be modified by the user to define any circuit, up to a total of nine different spans with nine parallel circuits. Different cable characteristic may be assigned to each span and circuit in addition to different earth resistor values. Normal operation and different types of short-circuits (single and three phase) may also be modeled at different points and situations. Various circuit currents and reduction factors can be considered for fault distance and other special configurations. Even, optionally, one can enter a description of the circuit that appears in the report that is generated during the simulation.

The number of segments and circuits can be set by the user. Most of the commands are clear and easy. Obviously, the button “Length” is used to indicate the span length, and so on. The different values of the sections can be configured, both regarding the segments and the circuits (Fig. 12).

Clicking on the button “Cable Parameters”, resistance of conductor and sheath, cable capacity, and outer radius of the sheath can be modified (Fig. 13). The same parameters can be set for the support cable.

In the “Section circuit” window one can select the coordinates of the cables of the circuit for the current segment (Fig. 14, left). Up to a maximum of two ecc may be entered for each circuit, and also the point where they are transposed as a fraction of 1 (the default transposal

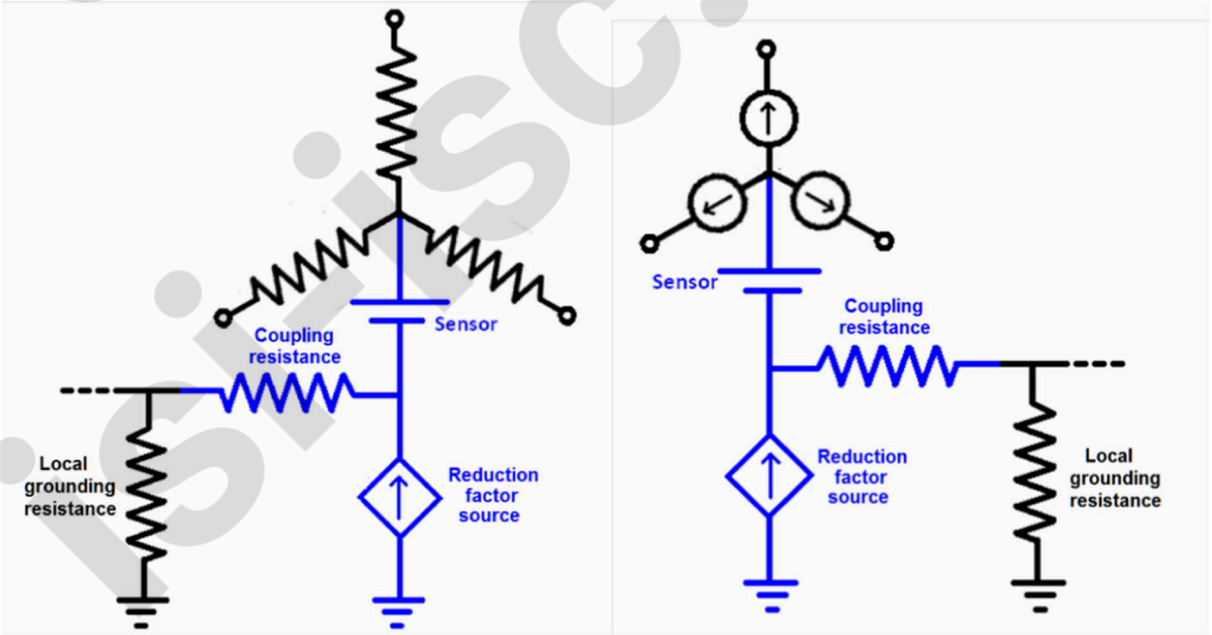

Fig. 11. Distant phase fault in semi-siphon (left) and siphon fault (right).

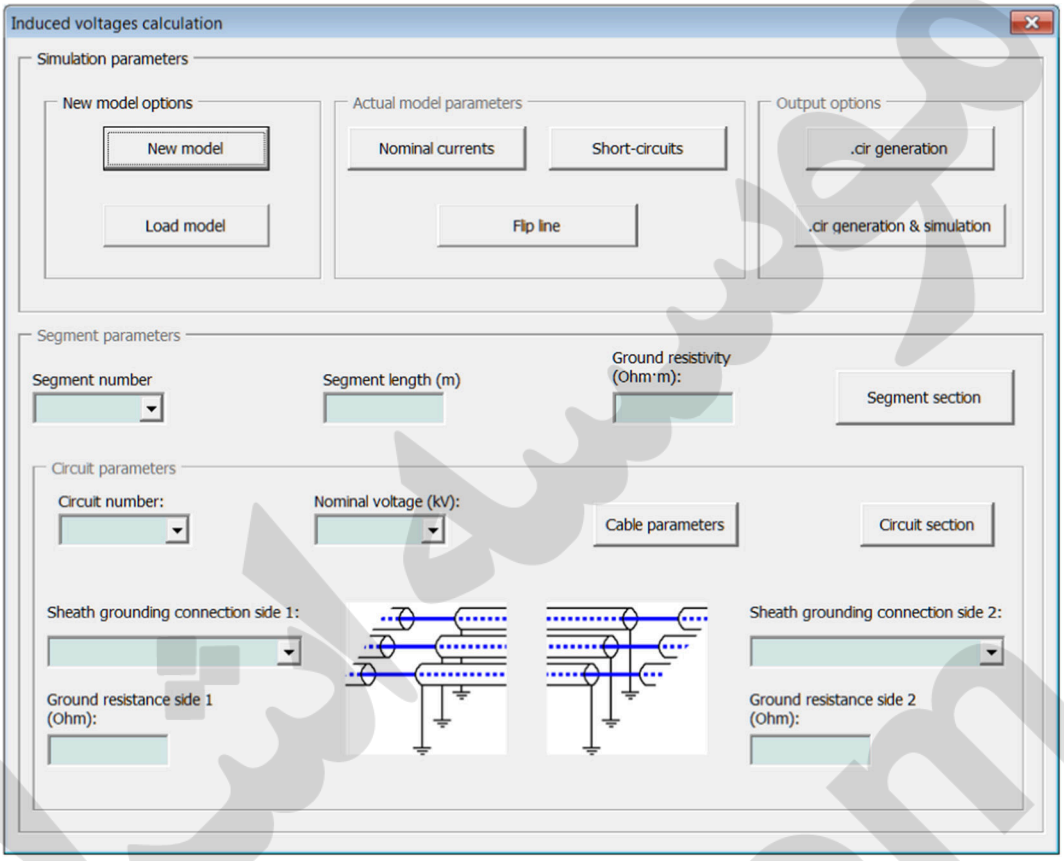

Fig. 12. Main software screen.

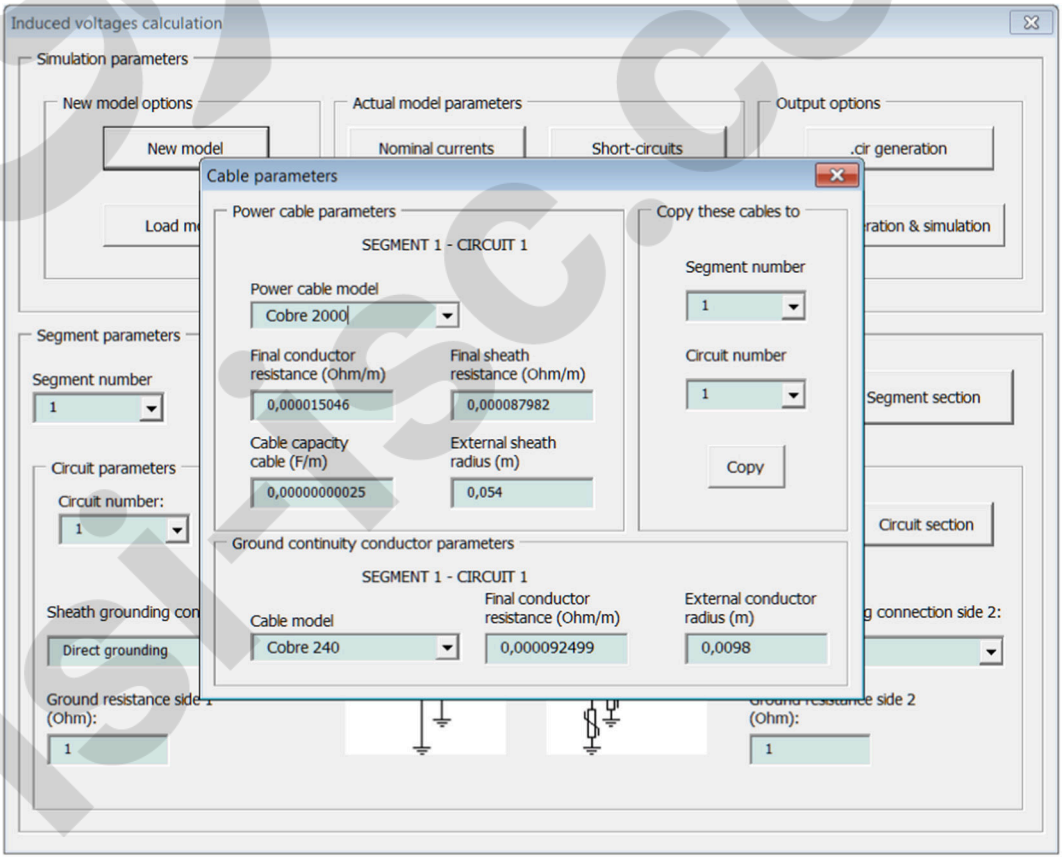

Fig. 13. Configuration of cable parameters.

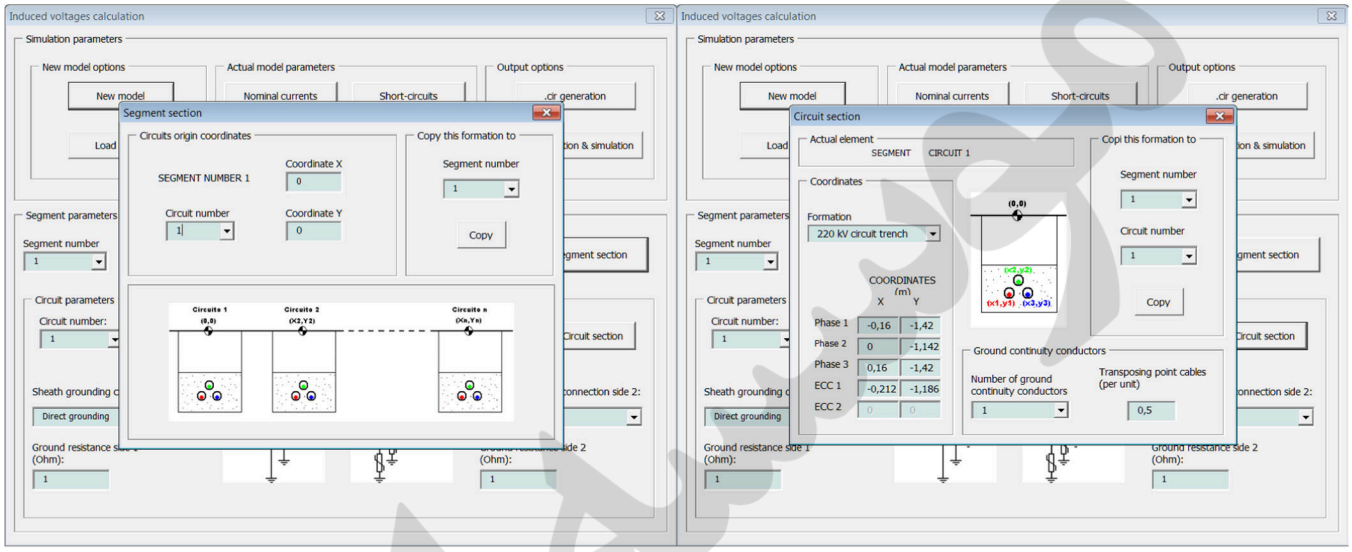

Fig. 14. Coordinates configuration of the different circuits and segments.

point is 0.5, that is, at halfway). Segment section button allows to change the reference coordinates of the different circuits (Fig. 14, right).

"Simulation Parameters" screen allows us to select the type of simulation (normal operation, three phase circuit, or the four different types of short circuits). It is also possible to select the circuit that is shorting, the current of the short circuit, and the reduction factors for distant failure and siphoning. The phase currents are also chosen for each circuit.

This way, it is easy to visualize the voltage or current at any point in the circuit. Even more, the user can easily see the terminal voltage of an arrester or the current passing through a sheath, or the voltage component in sheath 2 of circuit 1 resulting from the current flowing in sheath 3 of circuit 2, and so on.

The simulation tool shows a large number of comments that help the user to track it easily and, if needed, to make any necessary change quickly. The report that is generated is identified by the sheath and four digits, meaning the section, circuit, phase, and end point of the section, respectively. The measures of all the sheath RMS voltages are also indicated. This report has the following information.

- Circuit description, including segment, circuit and phase.
- Sheath description, indicating section, circuit, and uncharger if applicable.
- Support cable description, with information regarding the section, circuit and number of supporting cables (there may be one or two)
- Induced sources description, indicating the inductive element (wire or sheath, segment, circuit, phase) and the element that receives the induction (sheath, cable, segment, circuit, and phase).
- Power sources (current sources)
- Description of the loads (star resistors)
- Initial values of the different knots of the circuit.
- Description of the measures taken on sheaths.
- Other technical information.

4.1. Model validation with theoretical results

In order to test the simulator and to validate the model, a series of simulations were run under different configurations and compared to known results, the theoretical expected calculations, taking into account that the obtained values are approximate ones.

Fig. 15 shows the result of simulating the local voltages induced in the sheaths of a 220 kV single circuit. It consists of a span of 500 m with SP sheath connection with one ecc transposed to halfway, and operating normally. It can be seen that two sheaths have approximately the same amplitude of induced voltage and 120° offset (red[1] and blue lines). These sheaths correspond to the lowest phases in the trefoil formation. The ecc is only very close to them along half of the run.

However, the voltage induced in the central phase of the trefoil formation (magenta line) is smaller in magnitude. This is because the ecc is close to this phase throughout the segment and, therefore, this is the phase that induces more voltage over the ecc. That is why the ecc current is approximately in opposition of phase to the conductor current. Indeed, the component of the induced voltage in the central sheath caused by the ecc current is such that it lowers the overall magnitude of the induced voltage in this sheath, and it also increments it in the other two sheaths more than if there were no such current.

Once the simulator has been tested in general terms, seeing that it provides the expected results, two different cases have been simulated to validate the model.

(a) First case: segment of a single circuit

As a first example, the results of the simulation of a single circuit segment with solid bonding connection are analyzed. The test is performed on a 1 km line with a trefoil formation, with a distance of 250 mm between phases and various combinations of grounding resistance values. The results are given in V/kA (kA fault). We compared the theoretical results (Table 1) with the results provided by the software (Table 2) on the basis of a single-phase short-circuit and four different configurations. The theoretical expected results are obtained from [35], pp. 855–863, applying the following formulas.

Close fault in semi-siphon: the induced voltages in local ground (R1 and R2) in a SB connection, with a trefoil formation and without current through the other conductors, for a single-phase short circuit, are given by,

$$V_{R1} = -\varepsilon \cdot I_{cc} \cdot R_1$$

$$V_{R2} = \varepsilon \cdot I_{cc} \cdot R_2$$

$$\varepsilon = \frac{R_p}{3 \cdot (R_0 + R_1 + R_2) + R_p + jX_{cp} + 2 \cdot jX_m}$$

[1] For interpretation of color in Figs. 15–17, and 20, the reader is referred to the web version of this article.

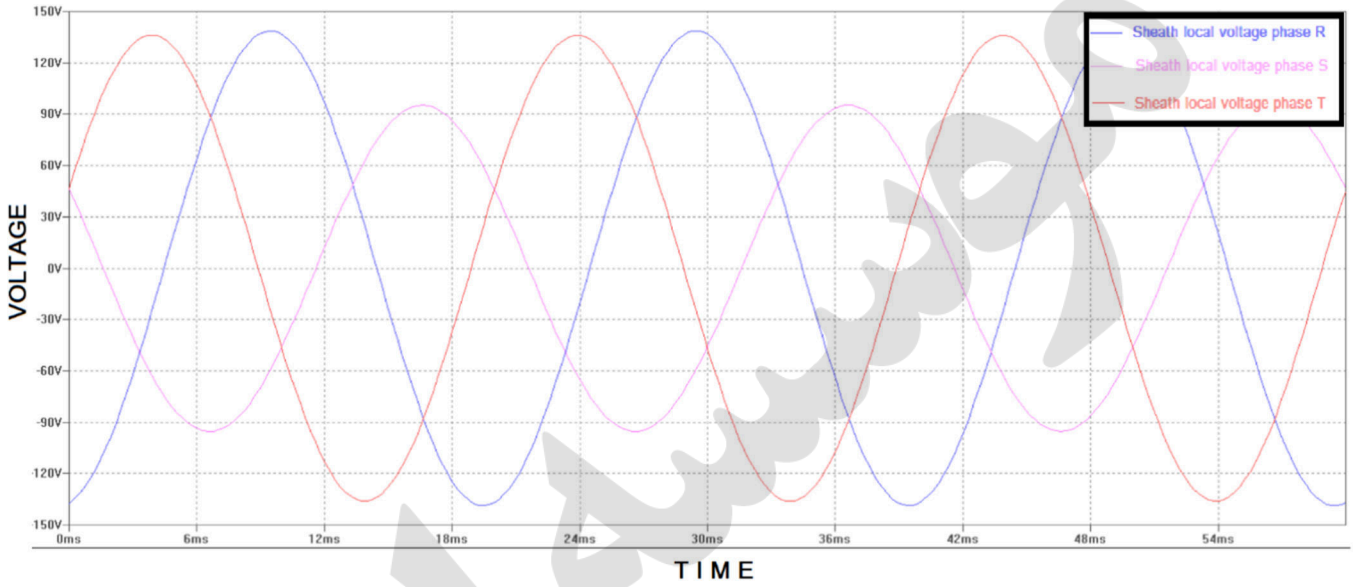

Fig. 15. Simulation of induced local voltages in the sheaths.

Table 1
Theoretical results.

L (km)	R1 (Ohm)	R2 (Ohm)	s (mm)	Close semi-siphon		Distant siphon		Distant semi-siphon		Close siphon	
1	0.25	0.25	250	−9.4	9.4	−172.7	172.7	−87.6	−196	196	87.6
1	0.25	0.5	250	−7.5	15.1	−138.6	277.1	−133.1	−314.4	195.3	140.5
1	0.5	0.5	250	−12.3	12.3	−227.6	227.6	−218.7	−320.8	320.8	218.7
1	0.25	10	250	−0.7	28.3	−13.3	532.5	−242.4	−604.2	243.3	269.9
1	0.5	10	250	−1.4	27.6	−26	519.9	−473.4	−732.9	475.1	499.6
1	10	10	250	−14.6	14.6	−274.2	274.2	−4993.1	−5010.6	5010.6	4993.1
1	10	20	250	−9.7	19.4	−183.1	366.1	−6657.9	−6690.9	6667	6667.6
1	20	20	250	−14.6	14.6	−274.8	274.8	−9994	−10007.8	10007.8	9994

Table 2
Simulation results.

L (km)	R1 (Ohm)	R2 (Ohm)	s (mm)	Close semi-siphon		Distant siphon		Distant semi-siphon		Close siphon	
1	0.25	0.25	250	−9.2	9.2	−172.3	172.3	−87.4	−195.5	195.5	87.4
1	0.25	0.5	250	−7.4	14.8	−138.2	276.4	−132.8	−313.8	194.9	140.2
1	0.5	0.5	250	−12.2	12.2	−227.1	227	−218.2	−320.2	320.2	218.2
1	0.25	10	250	−0.7	28.5	−13.3	531.6	−242	−603.6	242.8	269.7
1	0.5	10	250	−1.4	27.8	−26	519	−472.5	−732.3	474.2	498.9
1	10	10	250	−14.7	14.7	−274.3	273.3	−4983.7	−5001.5	5001.6	4983.8
1	10	20	250	−9.8	19.6	−183.5	365	−6645.7	−6679.2	6654.8	6655.2
1	20	20	250	−14.7	14.7	−275.4	273.5	−9975.4	−9989.5	9989.6	9975.5

V_{R1} → R1 voltage (V)
V_{R2} → R2 voltage (V)
I_{cc} → Short circuit current (A)
ε → Fault current fraction circulating on the ground (dimensionless)
R_0 → Induced resistance between conductor and sheath (Ω)
R_p → Sheath resistance (Ω)
X_{cp} → Induced reactance between conductor and sheath of the same cable (Ω)
X_m → Mutual reactance between conductor and shield of different cables (Ω)

The formulas for the short circuit type 2 in the same conditions as the previous one are the following.

Distant fault in semi-siphon.

$$V_{R1} = -R_1 \cdot (1 + \varepsilon) \cdot \frac{I_{cc}}{2}$$

$$V_{R2} = -R_2 \cdot (1 - \varepsilon) \cdot \frac{I_{cc}}{2}$$

$$\varepsilon = \frac{3 \cdot (R_2 - R_1 - R_0) + R_p - jX_{cp} - 2 \cdot jX_m}{3 \cdot (R_0 + R_1 + R_2) + R_p + jX_{cp} + 2 \cdot jX_m}$$

Close fault in siphon:

$$V_{R1} = R_1 \cdot (1 - \varepsilon) \cdot \frac{I_{cc}}{2}$$

$$V_{R2} = R_2 \cdot (1 + \varepsilon) \cdot \frac{I_{cc}}{2}$$

$$\varepsilon = \frac{3 \cdot (R_1 - R_2 - R_0) + R_p - jX_{cp} - 2 \cdot jX_m}{3 \cdot (R_0 + R_1 + R_2) + R_p + jX_{cp} + 2 \cdot jX_m}$$

Distant fault in siphon:

$$V_{R1} = -R_1 \cdot \varepsilon$$

Table 3
Relative error between simulation and theoretical results for a single circuit.

Close semi-siphon		Distant siphon		Distant semi-siphon		Close siphon	
−2.1%	−2.1%	−0.2%	−0.2%	−0.2%	−0.3%	−0.3%	−0.2%
−1.3%	−2.0%	−0.3%	−0.3%	−0.2%	−0.2%	−0.2%	−0.2%
−0.8%	−0.8%	−0.2%	−0.3%	−0.2%	−0.2%	−0.2%	−0.2%
0.0%	0.7%	0.0%	−0.2%	−0.2%	−0.1%	−0.2%	−0.1%
0.0%	0.7%	0.0%	−0.2%	−0.2%	−0.1%	−0.2%	−0.1%
0.7%	0.7%	0.0%	−0.3%	−0.2%	−0.2%	−0.2%	−0.2%
1.0%	1.0%	0.2%	−0.3%	−0.2%	−0.2%	−0.2%	−0.2%
0.7%	0.7%	0.2%	−0.5%	−0.2%	−0.2%	−0.2%	−0.2%

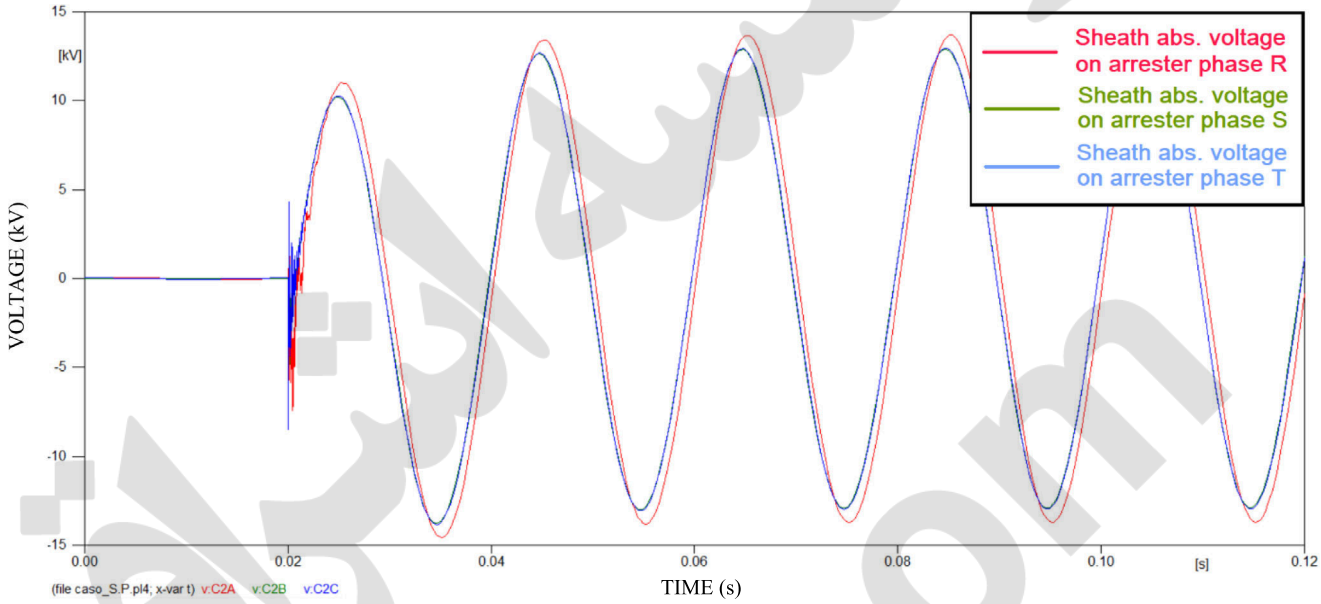

Fig. 16. Sheath absolute voltages on the arresters side (ATP simulation).

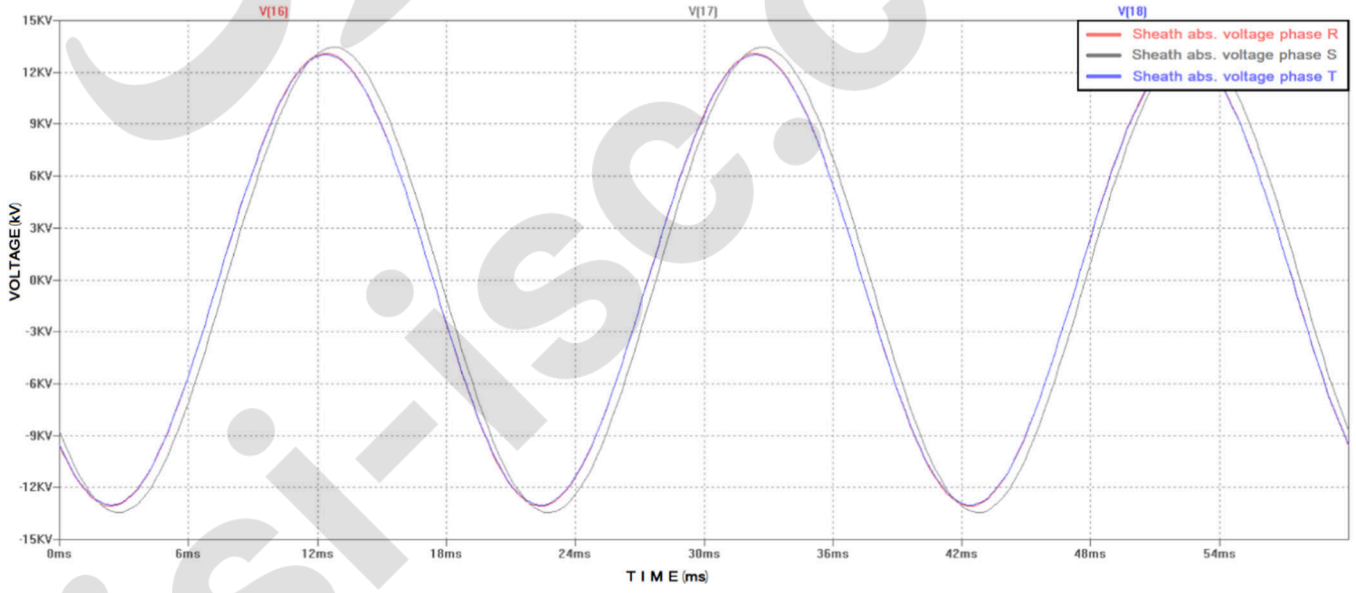

Fig. 17. Sheath absolute voltages on the arresters side (proposed simulation tool).

$$V_{R2} = R_2 \cdot \varepsilon$$

$$\varepsilon = \frac{-3 \cdot R_0 - jX_{cp} - 2 \cdot jX_m}{3 \cdot (R_0 + R_1 + R_2) + R_p + jX_{cp} + 2 \cdot jX_m}$$

The average error between them, i.e., the difference between the theoretical and simulated value is 0.2% (Table 3). The error is very small for every combination of grounding resistors and for all types of short-circuit, thereby underlining the reliability of the program and the modeling methodology.

It should also be noted that the theoretical calculation does not take

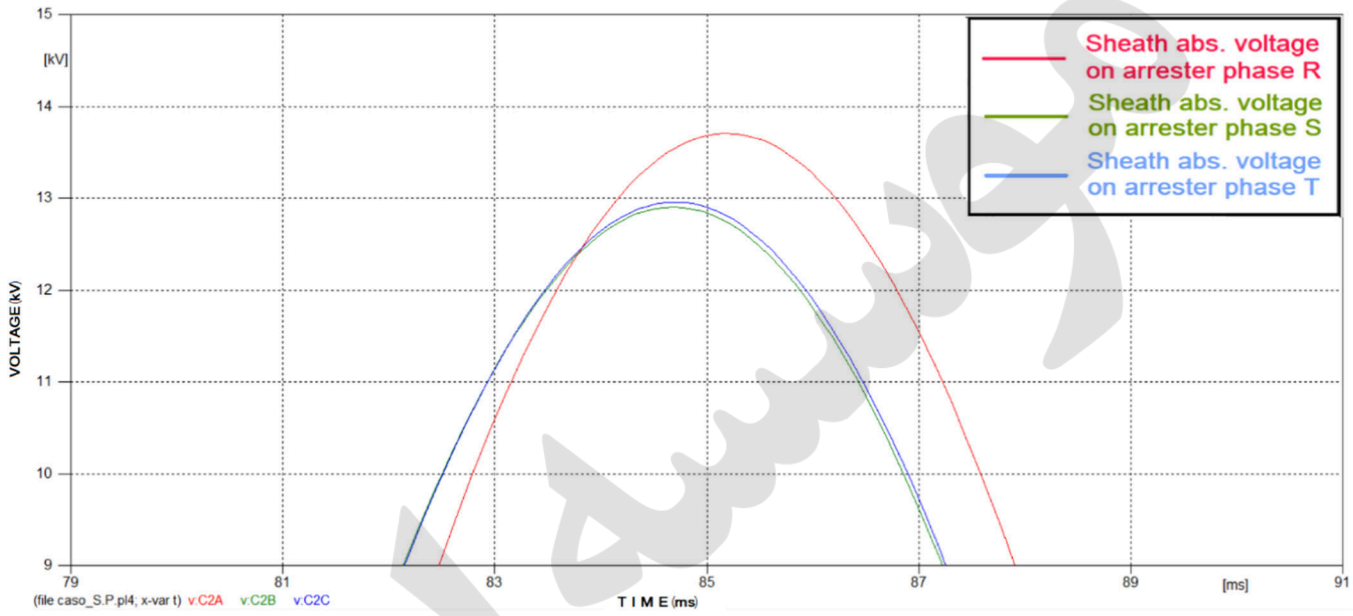

Fig. 18a. Detail of the absolute voltages peaks of the three sheaths on the arrester side obtained with ATP.

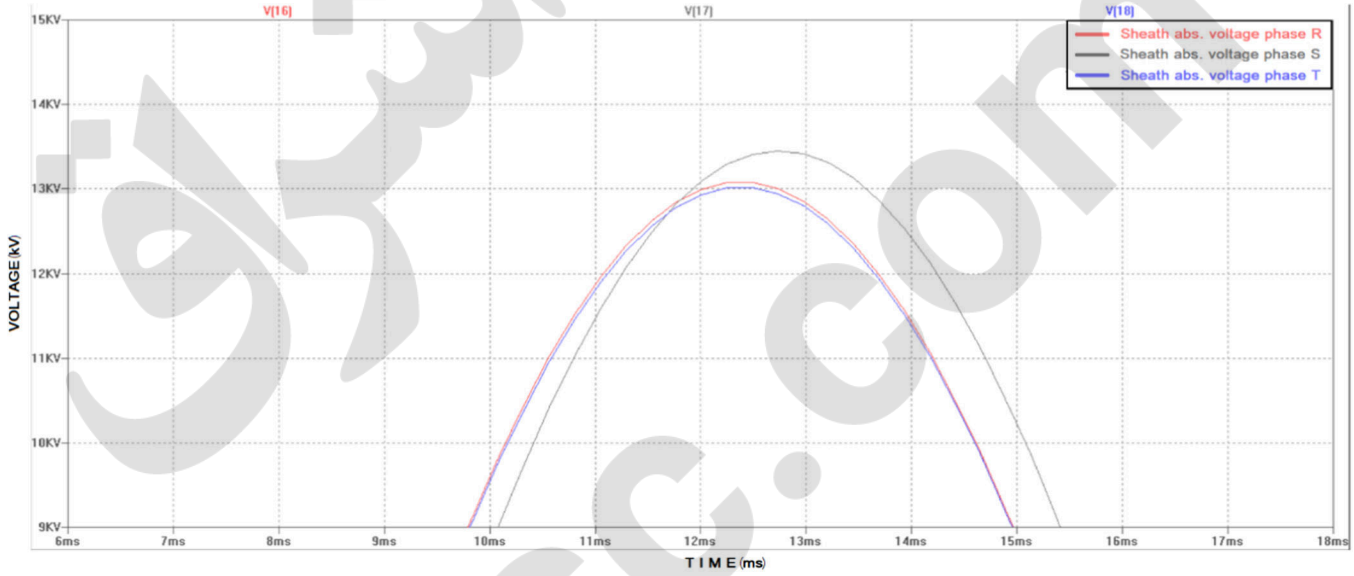

Fig. 18b. Detail of the absolute voltages peaks of the three sheaths on the arrester side obtained with our proposed simulator.

into account the existence of capacitors although the model does. Its influence on the results is low since it only involves small currents, but the lower the induced voltage results the more noticeable it becomes.

4.2. Model validation with other simulator results

In order to further validate the model and the developed tool, simulations have been also performed using the commercial and well known ATP software and the results are compared to those obtained by our simulator.

First, a simple 66 kV real circuit with a 655 m section in single point (SP) has been simulated. The underground cable is made of aluminum with a 1000 mm^2 section and a copper sheath of 95 mm^2. Previous studies revealed that in the event of a short circuit in one of the substations, a current of 20 kA can be generated. The absolute value of the voltages on the three sheaths on the arresters side are shown in Fig. 16 (with ATP) and in Fig. 17 with our software.

In Fig. 17, V[16] (red line), V[17] (grey line) and V[18] (blue line) are the absolute sheath voltages on the side of the arresters. It is possible to see how the maximum induced voltage occurs in the sheath of the cable in short circuit (cable 2, the upper one in the trefoil formation). That is, V[17] in Fig. 17, obtained with our program, and v.C2A (red line) in Fig. 16, obtained with the ATP simulation.

The other two sheaths (those of cables 1 and 3) have an induced voltage practically identical between them and slightly lower than the phase of the one that suffers the short circuit. The induction is lower because they are at a greater distance from the conductor short-circuited than the sheath of cable 2.

Although it is not possible to overlap both figures, it can be seen that the values of voltage and phase shifts are quite similar for the ATP and our simulation tool. The measures are almost identical.

Indeed, if we represent with more detail the sheath voltages (Figs. 18a and 18b), the differences between the results obtained by the ATP (Fig. 18a) and the simulator proposed in this work (Fig. 18b) are minimum.

Besides, in Figs. 18a and 18b it is possible to see the three voltage

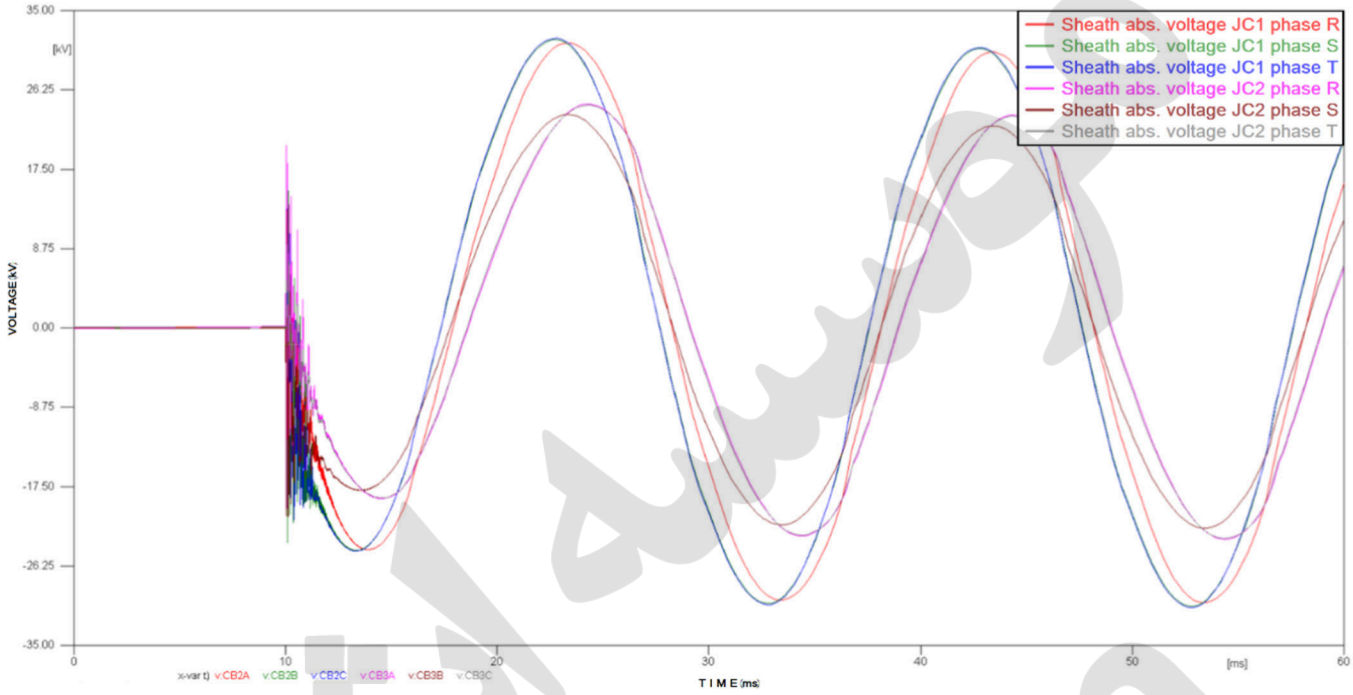

Fig. 19. Sheath absolute voltages in both junction chambers (ATP).

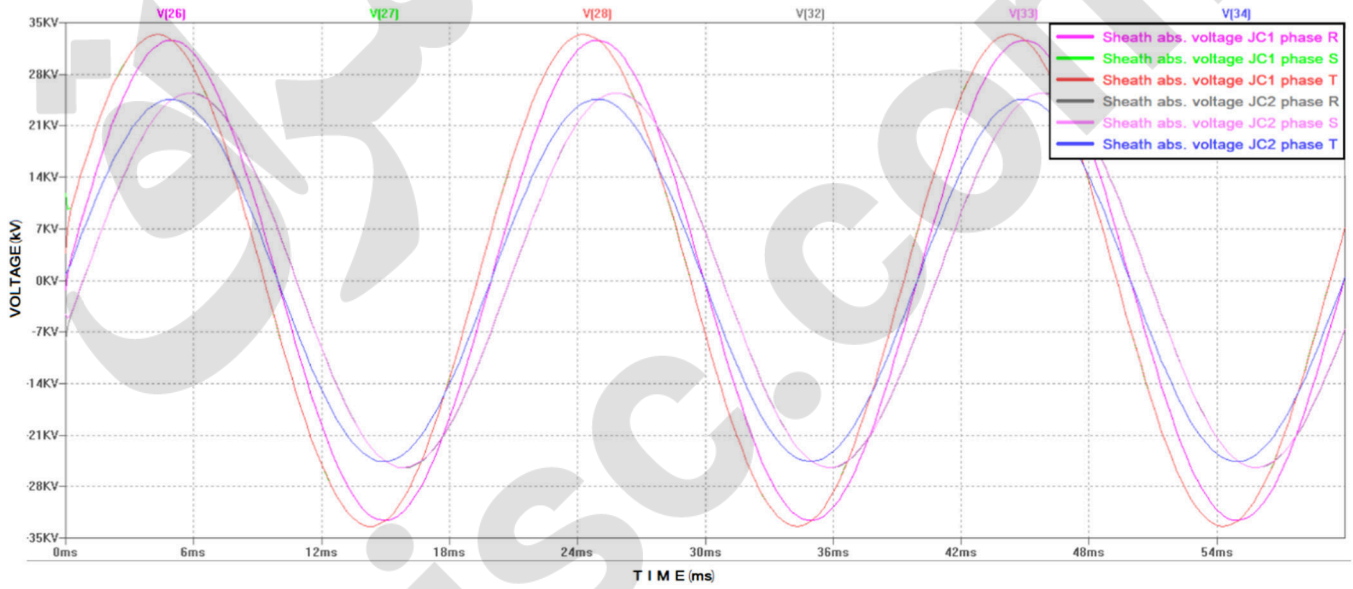

Fig. 20. Sheath absolute voltages in both junction chambers (proposed simulator).

lines. In the previous figures, both for the ATP and our simulation, one of the voltages was overlapped and could not been seen.

Our simulator has also been compared with ATP for a more complex circuit, an underground 132 kV real line with a simple circuit, cross bonding (CB) grounding and trefoil formation with phase distant of 200 mm. The line consists of three CB sections with 1060 m, 1135 m and 1165 m length, respectively. The resistance of the sheath at 90° is 87.9 μΩ/m and its radius is 5.4 cm. Grounding resistors in the substations are set to 1 Ω, whereas in the intermediate junction chambers are set to 5 Ω.

Simulation is carried out for a single phase siphon short circuit close to 40 kA. Fig. 19 shows the absolute voltages on the sheaths obtained in each one of the two junction chambers, by the ATP simulator.

The absolute voltages for the same scenario, obtained with the program developed in this work, can be seen in Fig. 20, using the same time and voltage scales.

Fig. 20 shows two groups of three absolute voltages. The group of the three major voltages corresponds to V[26] (pink line), V[27] (green line) and V[28] (red line); the last two are difficult to see because they are overlapped. These are the voltages of the sheaths in the first splice chamber; that is, on the side furthest from the short circuit, as expected and as with ATP.

The other group of the three voltages, V[32], V[33] and V[34] (grey, magenta and blue lines, respectively), represents the absolute voltages in the sheaths of the junction chamber closest to the short circuit.

Again, as in the previous case, the values obtained by the ATP simulator and our proposal are the same.

This allows us to validate the modeling and the developed simulator.

5. Conclusions and future work

The modeling carried out in this work is quite consistent with reality in terms of modeling the underground line with all the parameters that play an important role in calculating the induced voltages.

Unlike other proposals [36], this way of modeling allows greater speed of development because it is dynamic and the model itself does not appear in SPICE language until the end. If an element by element modeling is performed using a graphical environment (like Simulink or other graphics-based environments such as Schematics SPICE) it is not possible to connect a line with another efficiently if you do not have a module for a dual circuit. Obviously, this applies to a triple circuit, quad circuit, etc.

Although some newer versions of certain simulators allow the possibility of coupling multiple circuits, it is at the expense of laboriously defining each connection manually, a task performed automatically by our software.

For this reason, it is common in professional environments to see a single circuit line being modeled instead of two lines (when applicable) with the assumption that having a double circuit will not change the induced voltages in the first circuit in the event of a short circuit. Although this may be a common case, it may be of interest to know exactly what happens, or to ascertain the voltage induced in the sheaths or the circuit that does not have the fault. Those eventualities are covered by the software developed in this work.

As future work, combining the steady state behavior and the transient response of the circuit could be an interesting approach. Another possible extension of our work will be to apply Multiconductor Cell Analysis (MCA) [37], to deal with the variables computation in faulty occurrences. Indeed, MCA considers the proximity effect for steady state [38,39].

Acknowledgments

Authors would like to thank the anonymous reviewers for the useful comment and suggestions that have helped to improve the manuscript.

Funding sources

This research did not receive any specific grant from funding agencies in the public, commercial, or not-for-profit sectors.

References

[1] Valle Y, Hampton N, Perkel J, Riley C. Underground cable systems. Electrical transmission systems and smart grids. Springer; 2013. p. 195–237.
[2] Lee JB, Jung CK. Technical review on parallel ground continuity conductor of underground cable systems. J Int Counc Electr Eng 2012;2(3):250–6.
[3] Jung CK, Lee JB, Wang Kang JWX, Song YH. Characteristics and reduction of sheath circulating currents in underground power cable systems. Int J Emerg Electr Power Syst 2004;1(1):1–17.
[4] Tziouvaras DA, Needs J. Protection of mixed overhead and underground cable lines. In: 12th IET int conf on developments in power system protection; 2014. p. 1–6.
[5] Sheng B, Zhou C, Dong X, Hepburn DM, Alkali B, Zhou W. PD detection and localisation in cross-bonded HV cable systems. In: 22nd int. conf. and exhibition on electricity distribution; 2013. p. 0129.
[6] Lafaia I, Yamamoto Y, Ametani A, Mahseredjian J, de Barros MTC, Kocar I, et al. Propagation of intersheath modes on underground cables. Electr Power Syst Res 2016;138:113–9.
[7] Akbal B. Determination of the sheath current of high voltage underground cable line by using statistical methods. Int J Eng Sci Comput 2016;6(3):2188–92.
[8] Jung CK, Lee JB, Kang JW. Sheath circulating current analysis of a cross bonded power cable systems. J. Electr Eng Technol 2007;2(3):320–8.
[9] Gudmundsdottir US, Gustavsen B, Bak CL, Wiechowski W. Field test and simulation of a 400-kv cross-bonded cable system. IEEE Trans Power Delivery 2011;26(3):1403–10.
[10] Gudmundsdottir US. Proximity effect in fast transient simulations of an underground transmission cable. Electr Power Syst Res 2014;115:50–6.
[11] Asada T, Baba Y, Nagaoka N, Ametani A, Mahseredjian J, Yamamoto K. A study on basic characteristics of the proximity effect on conductors. IEEE Trans Power Delivery 2017;32(4):1790–9.
[12] Brito AI, Machado VM, Almeida ME, das Neves MG. Skin and proximity effects in the series-impedance of three-phase underground cables. Electr Power Syst Res 2016;130:132–8.
[13] Herrera-Orozco AR, Bretas AS, Orozco-Henao C, Iurinic LU, Mora-Flórez J. Incipient fault location formulation: a time-domain system model and parameter estimation approach. Int J Electr Power Energy Syst 2017;90:112–23.
[14] Gustavsen B, Bruaset A, Bremnes JJ, Hassel A. A finite-element approach for calculating electrical parameters of umbilical cables. IEEE Trans Power Delivery 2009;24(4):2375–84.
[15] Pagnetti A, Xemard A, Paladian F, Nucci CA. An improved method for the calculation of the internal impedances of solid and hollow conductors with the inclusion of proximity effect. IEEE Trans Power Delivery 2012;27(4):2063–72.
[16] Patel UR, Gustavsen B, Triverio P. An equivalent surface current approach for the computation of the series impedance of power cables with inclusion of skin and proximity effects. IEEE Trans Power Delivery 2013;28(4):2474–82.
[17] Patel UR, Gustavsen B, Triverio P. Proximity-aware calculation of cable series impedance for systems of solid and hollow conductors. IEEE Trans Power Delivery 2014;29(5):2101–9.
[18] Chen H, Du Y. Proximity effect in transient analysis of radio base stations. Int J Numer Model Electr Netw Dev Fields 2018:e2335.
[19] Shaban M, Salam MA, Ang SP, Voon W. Induced sheath voltage in power cables: a review. Renew Sustain Energy Rev 2016;62:1236–51.
[20] Ben-Amar TAF, Abdallah HH. Fault prelocalization of underground single-phase cables: modeling and simulation. Int J Electr Power Energy Syst 2013;44(1):514–9.
[21] Jung CK, Jung YH, Kang JW. A study on lightning overvoltage characteristics of grounding systems in underground distribution power cables. J Electr Eng Technol 2014;9(2):628–34.
[22] Aloui T, Amar FB, Abdallah HH. Fault prelocalization of underground single-phase cables: modeling and simulation. Int J Electr Power Energy Syst 2013;44(1):514–9.
[23] Jensen CF, Nanayakkara OMKK, Rajapakse AD, Gudmundsdottir US, Bak CL. Online fault location on AC cables in underground transmission systems using sheath currents. Electr Power Syst Res 2014;115:74–9.
[24] Todorovski M, Ackovski R. Equivalent circuit of single-core cable lines suitable for grounding systems analysis under line-to-ground faults. IEEE Trans Power Delivery 2014;29(2):751–9.
[25] Czapp S, Dobrzynski K, Klucznik J, Lubosny Z. Computer-aided analysis of induced sheath voltages in high voltage power cable system. In: IEEE 10th int conf on digital technologies; 2014. p. 43–9.
[26] Ametani A. A general formulation of impedance and admittance of cables. IEEE Trans Power Apparatus Syst 1980;3:902–10.
[27] Patel UR, Triverio P. MoM-SO: a complete method for computing the impedance of cable systems including skin, proximity, and ground return effects. IEEE Trans Power Delivery 2015;30(5):2110–8.
[28] Linear Technology LT Spice IV User's Guide. Milpitas, CA: Linear Technology; 2011.
[29] CIGRE Task Force. B1.26. Earth potential rises in specially bonded screen systems. Brochure 347 2008.
[30] Benato R, Colla L, Sessa SD, Marelli M. Review of high current rating insulated cable solutions. Electr Power Syst Res 2016;133:36–41.
[31] Vijayaraghavan G, Brown M, Barnes M. Practical grounding, bonding, shielding and surge protection. Butterworth-Heinemann; 2004.
[32] Grainger JJ, Stevenson WD. Análisis de Sistemas de Potencia. México: McGraw-Hill; 1996.
[33] Working Group 07 of Study Committee 21. Guide to the protection of specially bonded cable systems against sheath overvoltages. Electra; 1990. p. 128.
[34] IEEE, Guide for the application sheath-bonding methods for single conductor cables and calculation of induced voltages and currents in cable sheaths. ANSI-IEEE Std. 575; 1988.
[35] Simón P, Garnacho F, Moreno J, González A. Cálculo y diseño de líneas eléctricas de alta tensión. Madrid, Spain: Garceta; 2011.
[36] Aloui T, Amar FB, Derbal N, Abdallah HH. A method of prelocalization improvement of resistive faults affecting long single-phase underground cables: analytical and numerical calculation. IJ-STA, vol. 5, no., 1; 2011. p. 1448–57.
[37] Benato R. Multiconductor analysis of underground power transmission systems: EHV AC cables. Electr Power Syst Res 2009;79(1):27–38.
[38] Benato R, Sessa SD, Guglielmi F, Partal E, Tleis N. Ground return current behaviour in high voltage alternating current insulated cables. Energies 2014;7(12):8116–31.
[39] Benato R, Sessa SD, De Zan R, Guarniere MR, Lavecchia G, Labini PS. Different bonding types of Scilla-Villafranca (Sicily–Calabria) 43-km Double-Circuit AC 380-kV Submarine-Land Cables. IEEE Trans Ind Appl 2015;51(6):5050–7.